CZECH TECHNICAL
UNIVERSITY
IN PRAGUE

FACULTY
OF MECHANICAL
ENGINEERING

DOCTORAL THESIS STATEMENT

CZECH TECHNICAL UNIVERSITY IN PRAGUE

FACULTY OF MECHANICAL ENGINEERING

DEPARTMENT OF MECHANICS, BIOMECHANICS AND MECHATRONICS

DOCTORAL THESIS STATEMENT

CLINICAL BIOMECHANICS OF UPPER EXTREMITY

by

Ing. Adam Kratochvíl

Doctoral Study Programme: Mechanical Engineering

Study Field: Biomechanics

Supervisor: prof. RNDr. Matej Daniel, Ph.D.

Doctoral thesis statement to obtain the academic title "Ph.D."

Prague 2024

Název česky: Klinická biomechanika horní končetiny

Disertační práce byla vypracována v kombinované formě doktorského studia na Ústavu mechaniky, biomechaniky a mechatroniky Fakulty strojní ČVUT v Praze.

Disertant: Ing. Adam Kratochvíl
Ústav mechaniky, biomechaniky a mechatroniky, Fakulta strojní ČVUT v Praze
Technická 4, 166 00, Praha 6, adam.kratochvíl@fs.cvut.cz

Školitel: prof. RNDr. Matej Daniel, Ph.D.
Ústav mechaniky, biomechaniky a mechatroniky, Fakulta strojní ČVUT v Praze
Technická 4, 160 00, Praha 6, Matej.Daniel@fs.cvut.cz

Oponenti doc. MUDr. Eduard Šťastný, Ph.D., 2. lékařská fakulta University Karlovy
doc. Ing. Luděk Hynčík, Ph.D., Nové technologie – výzkumné centrum Západočeské university v Plzni
doc. Ing. Aleš Jíra, Ph.D., Fakulta stavební ČVUT v Praze

Teze byly rozeslány dne: ....

Obhajoba disertace se koná dne .... v ……… hod.

v zasedací místnosti č. 623 (6. patro) Fakulty strojní ČVUT v Praze, Technická 4, Praha 6 před komisí pro obhajobu disertační práce ve studijním oboru Biomechanika.

S disertací je možno se seznámit na oddělení vědy a výzkumu Fakulty strojní ČVUT v Praze, Technická 4, Praha 6.

prof. RNDr. Matej Daniel, Ph.D.

předseda oborové rady oboru Biomechanika

Fakulta strojní ČVUT v Praze.

Annotation

This thesis introduces a comprehensive biomechanical analysis of reverse total shoulder arthroplasty (RTSA), incorporating both the shift of the center of rotation (COR) and humerus prolongation. The analysis is conducted using an innovative validated method based on widely available clinical data from preoperative and postoperative examinations of RTSA patients. We demonstrated that the magnification of plain radiographs in the shoulder region significantly varies among patients, with a mean value approaching 12%, which significantly differs from the commonly used 5%. Musculoskeletal geometry alterations are assessed through preoperative and postoperative X-rays, along with preoperative CT scans. An original method for evaluating COR shift in RTSA, based on postoperative X-rays, was introduced, and subsequently employed to determine the actual humerus prolongation. The findings unveiled an average actual humerus prolongation of 15.2 mm, that has not been previously reported. The influence of various musculoskeletal changes in RTSA was extensively examined and their impact on muscle forces and glenohumeral joint load was evaluated. Furthermore, a safe zone for humerus prolongation to prevent overloading the glenohumeral joint in RTSA was established, a crucial consideration for surgical procedures.

Keywords: biomechanics; shoulder; musculoskeletal model; Hill-type muscle model; reverse total shoulder arthroplasty; radiographical magnification; humerus prolongation; joint load.

Anotace

Tato disertační práce představuje komplexní biomechanickou analýzu reverzní náhrady ramenního kloubu, zahrnující jak posun centra rotace, tak prodloužení humeru. Analýza je provedena pomocí vlastní validované metody založené na běžně dostupných klinických datech z předoperačních a pooperačních vyšetření pacientů s totální endoprotézou ramene. Jedním z cílů, bylo prokázat, že zvětšení rentgenu v oblasti ramene je větší než v klinické praxi běžně používaných 5 % a že se mezi pacienty významně liší. Tato hypotéza byla potvrzena naměřenou průměrnou hodnota zvětšení blížící se 12 % s rozsahem od 5 % do 20 %. Změny v muskuloskeletální geometrii byly vyhodnoceny pomocí předoperačních a pooperačních rentgenových snímků spolu s předoperačním CT. Na základě pooperačních rentgenových snímků byla také zavedena nová metoda pro hodnocení posunu centra rotace u pacientů s reverzní endoprotézou ramene. Toto posunutí centra rotace bylo následně použito ke stanovení skutečného prodloužení humeru, jehož průměrná hodnota byla vyhodnocena jako 15,2 mm. Jedná se o rozměr, který nebyl nikdy dříve publikován. Dále byly vyhodnoceny jednotlivé změny muskuloskeletální geometrie a jejich vliv na svalové síly a zatížení ramene. Na závěr byla stanovena bezpečná zóna pro prodloužení humeru tak, aby se zabránilo přetížení glenohumerálního kloubu, což je zásadním hlediskem pro chirurgické výkony.

Klíčová slova: biomechanika; rameno; muskuloskeletální model; Hillův model svalu; reverzní náhrada ramene; radiografické zvětšení; prodloužení humeru; zatížení kloubu.

Contents

1 Introduction

Nearly every human activity is intricately connected to shoulder movement. Whether the shoulder serves as the primary actor in an activity or contributes to stability, such as in walking [1], its role is crucial. Shoulder joint movements are also integral to sports activities, contributing to both physical fitness and mental well-being [2]. However, shoulder biomechanics are highly complex, involving 4 joints (glenohumeral, acromioclavicular, scapulothoracic, and sternoclavicular) and 18 muscles working in synergy. Any disbalances in the shoulder complex can be a source of potential future complications [3].

Shoulder anatomy isn't inherently suited for an active life beyond 80 years, leading to problems that increasingly emerge with age, connected with reduced mobility and significant pain [4]. With the increasing life expectancy, which has nearly doubled in the last century in developed countries [5], and as the population ages [6], there is a growing demand to address pathological conditions affecting the shoulder. While less severe shoulder conditions, particularly in younger patients, such as impingement syndrome or soft tissue inflammation, can often be managed through conservative treatments [7], more serious degenerative conditions such as omarthrosis or rheumatoid arthritis, rotator cuff ruptures, or post-traumatic issues in older individuals may necessitate total shoulder arthroplasty (TSA) for joint mobility restoration [8].

Reverse total shoulder arthroplasty (RTSA), a procedure reversing the joint's anatomical arrangement, has become increasingly prevalent in addressing shoulder issues [9]. This reversal creates more favourable biomechanical conditions by shifting the center of rotation (COR) of the glenohumeral joint medially and slightly inferiorly and thus increasing the moment arm of deltoid muscle, which is the main mobilizer of the arm [10; 11]. This arrangement not even enhance mobility but also increasing stability of the joint by prestressing the shoulder muscles, especially benefiting patients with insufficient rotator cuff muscles [12].

The utilization of shoulder arthroplasty has witnessed significant expansion over the last decade, a trend supported by data from US databases. These statistics can be attributed, at least in part, to an aging population that aspires to maintain an active lifestyle [13]. In 2012, a total of 22,835 primary RTSA procedures were conducted [9]. In 2017, this number experienced a significant surge, nearly tripling to reach 62,705 RTSA procedures [9]. Over the same period, the count of anatomic total shoulder arthroplasty (TSA) procedures rose from 29,685 in 2012 to 40,665 in 2017 [9]. Conversely, the number of shoulder hemiarthroplasty procedures underwent a substantial decline, decreasing by almost half, from 11,695 in 2012 to 4,930 in 2017 [9].

To enhance the outcomes of RTSA, a thorough understanding of the biomechanical aspects of the resulting state is essential. While some characteristics can be measured from radiographs and other clinically available data of patients who have undergone RTSA [14], variables crucial to RTSA biomechanics, such as muscle forces, cannot be adequately assessed from these data alone. Hence, a comprehensive biomechanical analysis requires the utilization of mathematical musculoskeletal and muscle models. Therefore, the presented thesis deals with clinical biomechanics of shoulder with emphasis on modifications of glenohumeral geometry induced by reverse total shoulder arthroplasty.

2 State of the Art

2.1 Glenohumeral Joint

The glenohumeral joint is a part of shoulder complex (Fig. 1). It is the most mobile articulation within the human body [15]. The glenohumeral joint is synovial ball-and-socket joint, involving the coordinated action of 18 muscles and other structures such as the scapula and clavicle to provide full range motions with three rotational degrees of freedom (DOF) as well as three translational DOF [16]. In the specific context of the glenohumeral joint, the humeral head and the cavitas glenoidalis, forming the joint socket within the scapula, articulate with one another. Despite the partial widening of the fossa by the fibrous labrum glenoidale, it is important to note that the fossa's articular surface covers only a fraction, ranging from a quarter to a third of the humeral head's corresponding surface [17]. This anatomical feature permits a wide range of motion but, conversely, poses a potential source of dynamic instability [18].

Six fundamental movements can be described within the glenohumeral joint (Fig. 2). Full ranges of movements in glenohumeral joint are not isolated and depend on the movements of other joints in shoulder complex (Fig. 1) [18].

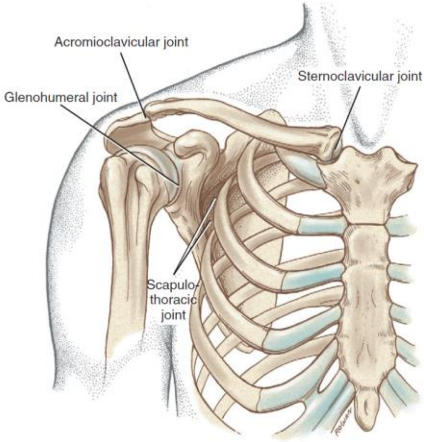

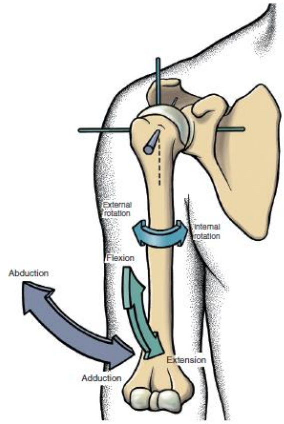

Fig. 1 Right shoulder complex [18]

Fig. 2 Fundamental movements in glenohumeral joint [18]

2.2 Reverse Total Shoulder Arthroplasty

Nowadays, total shoulder arthroplasty (TSA) is a common intervention for advanced glenohumeral joint osteoarthritis, demonstrating efficacy in terms of pain alleviation, functional enhancements, and a high rate of implant longevity in patients who maintain an intact rotator cuff [19]. On the other hand, RTSA has proven to be effective in reducing pain and optimizing functionality in patients with rotator cuff-deficient shoulders [20; 10]. Nevertheless, RTSA also serves as an effective treatment option for various other medical conditions. This includes the acute and delayed management of proximal humeral fractures [21], fracture malunion and non-union, cases of rheumatoid arthritis, tumor-related issues, fixed glenohumeral dislocation, revision arthroplasty [10] and severe glenoid bone wear [22].

In RTSA, the COR is medially and inferiorly shifted, influencing the biomechanical characteristics of the deltoid muscle (Fig. 3 and Fig. 4) and the remaining rotator cuff. The medialization of the COR elevates deltoid tension, crucial for prosthetic stability and improved efficacy during abduction [23]. Deltoid elongation, approximately 20% greater than that of a normal shoulder, is more pronounced in shoulders with cuff tear arthropathy. The abduction moment arm of the deltoid significantly increases by up to 40 mm, impacting its capacity to generate abductional forces [24]. The displacement of the humerus also affects the biomechanics of the remaining rotator cuff. In patients with cuff tear arthropathy, the supraspinatus and infraspinatus are frequently affected, resulting in compromised humeral rotation postoperatively [25]. Following conventional RTSA, rotational moment arms of the teres minor and subscapularis experience a substantial decrease. Muscle tension in these muscles decreases, and overall muscle length diminishes after surgery [26]. One potential strategy for mitigating these unfavorable biomechanical properties is to laterally shift the COR compared to conventional RTSA. However, it's important to note that this approach also addresses specific biomechanical disadvantages. Lateralized RTSA preserves rotational moment arms and prevents significant reductions in muscle tension for both the subscapularis and teres minor [27]. However, overall joint reaction forces in RTSA are reduced by approximately 30% compared to a normal shoulder, primarily in glenoid compression forces, while shear forces may increase with flexion [23].

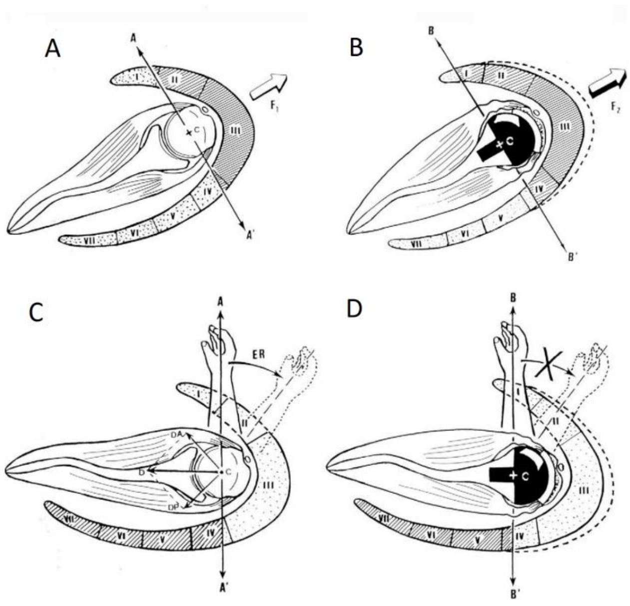

Fig. 3 In a normal shoulder, active elevation involves only the middle deltoid and a portion of the anterior deltoid segment (A); following RTSA, the medialization of COR engages more of the deltoid fibers for active elevation (B). Conversely, RTSA alters the dynamics in external rotation (ER), resulting in a reduced utilization of the posterior deltoid (D) compared to a normal shoulder (C). [11].

While the normal glenohumeral joint relies on dynamic stabilizers, such as the rotator cuff muscles, for stability, patients undergoing RTSA lack this natural dynamic stabilization. Consequently, maintaining the relative position of the humerus against the glenoid becomes crucial. The RTSA design strategically positions the convex surface on the glenoid and the concave surface on the humerus, effectively constraining the joint and preventing superior translation during deltoid contraction. This modification allows for a broader deviation angle of the joint force vector without the risk of dislocation. To enhance the stability of the RTSA, increasing the ratio between the diameters of the glenosphere and humeral socket is advocated [28]. Additionally, adjusting the depth of the humerosocket can contribute to stability, although this must be carefully balanced with the impingement-free range of motion [29].

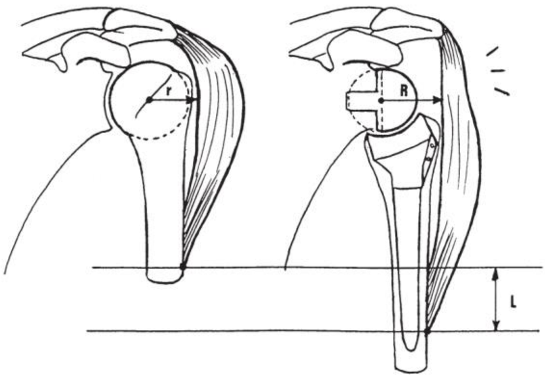

Fig. 4 The lever arm for deltoid contraction during elevation initiation is extended in RTSA due to the medialization of COR (R>r). Furthermore, the strength of the deltoid is increased by the prolonging of the humerus (L), leading to the elongation of deltoid fibers [11].

Another approach to boost deltoid efficiency is to pretension the muscle by increasing its resting length, achieved in the RTSA by distalizing the humeral insertion of the deltoid muscle (Fig. 26). Studies suggest that even a 1 cm distalization can yield an additional 30% efficiency [28]. This not only aids in deltoid torque production but also enhances joint stability. Optimal deltoid lengthening remains a subject of investigation, but studies indicate improved functional outcomes with arm lengthening rather than shortening [30].

2.3 Musculoskeletal models and in vivo measurements

The musculoskeletal modeling of the shoulder mechanism, which includes the thorax, clavicle, scapula, and humerus, is particularly challenging due to its complexity. Since the work of Inman et al., 1944 [31], various musculoskeletal mathematical models of the glenohumeral joint have been developed for clinical applications. Musculoskeletal models that specifically examine loading in the glenohumeral joint during abduction are compared in Fig. 5. The musculoskeletal models shown in Fig. 5 are Poppen and Walker, 1978 [32], van der Helm, 1994 [33], Favre et al., 2005 [34], Terrier et al., 2008 [35], and Anybody Shoulder model [36].

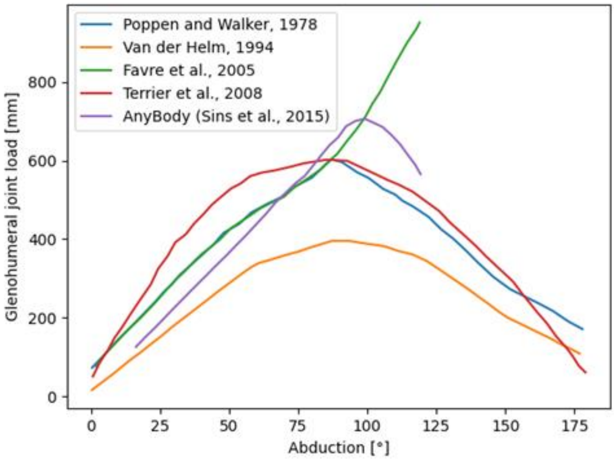

Fig. 5 Comparison of glenohumeral joint load during abduction in various musculoskeletal models. Data was obtained from [34] for Favre et al., 2005 and from [36] for the rest.

Bergmann et al., 2007 [37] adapted a clinically established shoulder implant (Biomodular, Biomet Inc., USA) to capture all six components of forces and moments exerted on the humeral head after shoulder hemiarthroplasty. The recorded data is conveniently accessible on the www.orthoload.com database, encompassing information from six subjects engaging in diverse activities within each patient. The resultant glenohumeral joint load during abduction for all 6 subjects is illustrated in Fig. 6. The group of subjects consisted of 3 males and 3 females, all right-handed with 5 right shoulder surgeries and one left. The average age of subjects at time of examination was 71 years (ranging from 63 to 81 years), the average weight was 83.5 kg (ranging from 50 to 103 kg) [38].

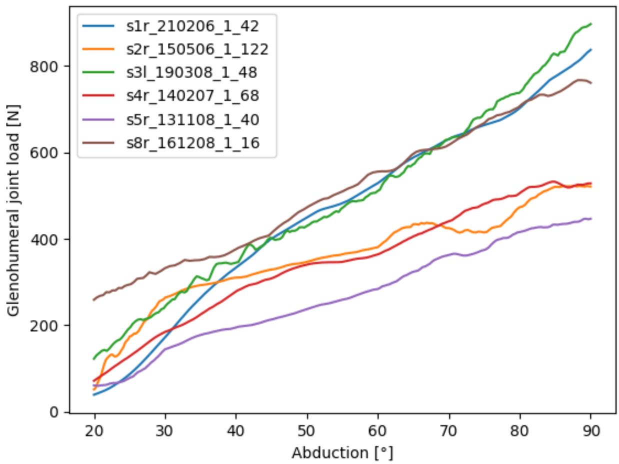

Fig. 6 In vivo measurments of glenohumeral joint load during abduction in six patients (s1–s5 + s8); r,l = right/left shoulder. Data is obtained from www.orthoload.com.

3 Aims of the thesis

Existing studies addressing RTSA predominantly focuses on clinical outcomes rather than conducting in-depth biomechanical analyses. In instances where biomechanical analysis is considered, it often emphasizes changes in COR while overlooking the significant aspect of humeral prolongation. Humeral prolongation is crucial in the biomechanical context as it induces prestressing of shoulder muscles, thereby influencing force patterns in the shoulder, alongside with the shift of COR.

Assessing changes in musculoskeletal geometry post-RTSA presents a complex challenge requiring specific clinical data. Many studies addressing musculoskeletal changes utilize custom-created data, such as full-arm X-rays, not standard in routine RTSA examinations. While preoperative and postoperative CT scans would be ideal, postoperative CT is not standard, necessitating the use of X-rays. In addition, the role of passive structures in musculoskeletal models of RTSA is usually neglected although it responds for joint stability. It is not clear whether and to which extend humeral lengthening contributes to overall joint load.

This dissertation aims to develop a comprehensive biomechanical analysis of RTSA, incorporating humeral prolongation and COR shift, utilizing widely available clinical data from preoperative and postoperative examinations of patients who have undergone RTSA. We hypothesize, that humeral prolongation along with the center of rotation change would reduce muscle forces and decrease joint loading.

Specific aim of the thesis is to develop an accurate method for evaluating musculoskeletal changes after RTSA based on routinely available clinical data, including preoperative CT and X-ray, along with postoperative X-ray. The initial step involves determining the precise magnification of X-rays, considering the hypothesis that the commonly used 5% magnification for shoulder radiographs may be higher and vary among patients. Secondly, a method must be devised to ascertain changes in musculoskeletal geometry, not just the shift of the COR but, crucially, the humeral lengthening after RTSA. This lengthening significantly influences muscle force ratios, impacting glenohumeral joint load and shoulder mobility. The method is applied in a clinical study and effect of patients' sex, weight, and age on the postoperative change in musculoskeletal geometry will be evaluated.

To understand glenohumeral joint load comprehensively, a musculoskeletal model of shoulder with a muscle model should be employed with modelling the muscles as Hill active units. Various Hill muscle models could be utilized to assess their impact on the resulting muscle force and glenohumeral load. We suggest that the formulations of the Hill-type models will considerably influence predicted glenohumeral load. The appropriate model should be verified to experimental measurements. Based on parametric analysis of RTSA surgery, a "safe zone" for humeral lengthening during RTSA could possibly be defined. We expect that the safe zone will indicate the permissible amount of humeral elongation during surgery without overloading the glenohumeral joint and its structures.

4 Methods

4.1 Radiographical Magnification in Shoulder Joint Region

A retrospective study included patients that have previously undergone total glenoid arthroplasty at the Motol University Hospital, Czechia. The implants analysed included only SMR Reverse Shoulder System (Lima Corporate, San Daniele del Friuli, Italy). The inclusion criteria for the study were as follows: unilateral RTSA, documented implant size and type, documented patient height and weight, digital AP (anterior-posterior) radiographs of the shoulder in neutral position obtained from archives, completely visible humeral and glenoid component of RTSA. The final cohort included 94 patients (62 female and 32 male). The average age of patients at time of surgery was 69,4 years (± 8,7 years, range 38 – 85 years). The data were collected during period spanning from 2014 to 2017.

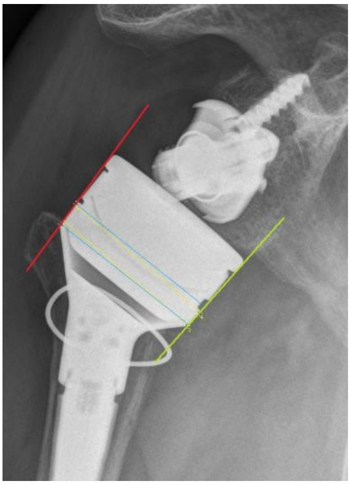

Fig. 7 Estimation of reverse humeral body dimension from standard AP shoulder radiograph. The lateral edge (highlighted in red) and the medial edge (highlighted in yellow) of the component were defined. The transverse size of the humeral body was determined as the mean perpendicular distance between the edges [I].

The diameter of the proximal part of reverse humeral body (component no. 1352.20.010) was used as reference (Fig. 7). The component is cylindrical in shape and its diameter is hence invariant to internal or external rotation. The cylindrical geometry was verified by fitting a cylinder to 3D scan of nonimplanted specimen using optical coordinate measuring system (Omnilux, RedLux Ltd, Romsey, UK). The physical diameter of 36.6 mm was obtained from cylindrical fit and confirmed by measuring of component using digital calliper (Mahr GmbH, Göttingen, Germany). The component dimension on radiograph was estimated from DICOM files using Fiji platform for biological-image analysis as follows: two points on each side of cylinder portion of the component were defined and used to construct the lateral and the medial edge of the component. A custom Matlab script (Matlab R2020b, The Mathworks, Inc., Natick, MA, USA) was programmed to calculate the diameter of the component as a mean perpendicular distance between the lines measured at defined points (Fig. 7). One observer (A.K.) analysed all radiographs. To assess the validity of the method for radiographic magnification estimation, five independent and blinded observers (postgraduate students of biomechanics at CTU in Prague) analysed a set of 20 randomly selected radiographs [I, V].

The radiographic magnification (*M*) of the implants was calculated as shown in equation (1).

$$M[\%] = \left(\frac{measured\ dimension}{true\ dimension} - 1\right) \cdot 100\% \qquad (1)$$

4.2 Determination of Changes in Musculoskeletal Geometry after RTSA

Identifying changes in musculoskeletal geometry for patients undergoing RTSA poses a significant challenge. The surgical procedure involves a medial and inferior shift in the COR of the glenohumeral joint, accompanied by humerus lengthening. These alterations impact strength ratios in shoulder muscles, thereby influencing mobility, range of motion, stability, and the lifespan of the replaced joint. To address this complexity, we have devised a semi-automatic method utilizing preoperative and postoperative X-rays, along with a preoperative computed tomography scan (Fig. 8). Our method was validated through virtual surgeries. Additionally, a sensitivity analysis was conducted.

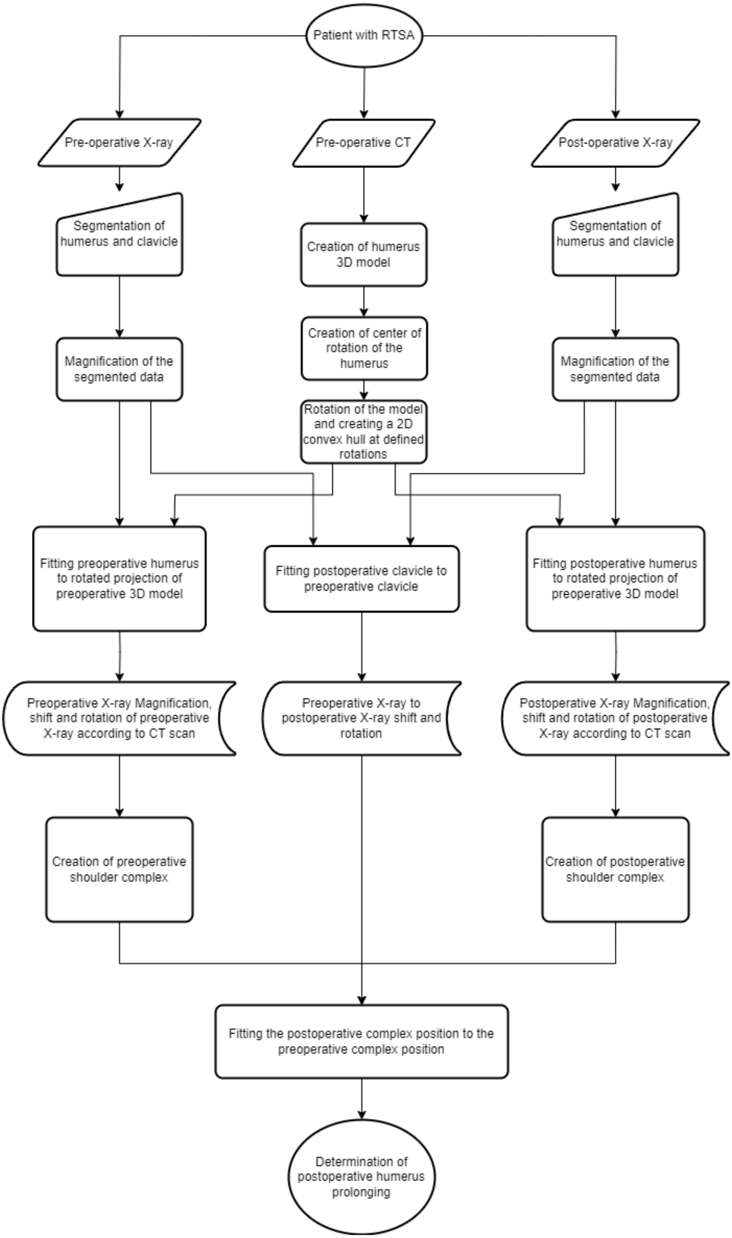

Fig. 8 Workflow diagram of method for determination of changes in musculoskeletal geometry after RTSA

Establishing the resection line poses a significant challenge as it varies among patients and affects humeral lengthening determination. Standard preoperative and postoperative anteroposterior radiographs may not provide a clear view, considering the fixed arm position postoperatively and thus unknown rotation in the shoulder. To address this, we utilized preoperative CT scans alongside X-rays. The 3D model created from the CT scan can be rotated to match the humerus positions in preoperative and postoperative X-rays, facilitating a cohesive comparison. Another challenge is X-ray magnification variation between preoperative and postoperative states, potentially introducing errors. To mitigate this, our method determines radiographical magnification in the shoulder joint. This involves estimating postoperative X-ray magnification using a replacement as a reference object, followed by evaluating preoperative magnification by aligning the preoperative clavicle contour with the postoperative clavicle contour.

A total of 34 patients who underwent RTSA at the Faculty Hospital in Motol, performed by one of six senior surgeons, were included. The study spanned the period between 2012 and 2020. Three patients were excluded due to suboptimal radiographic quality, resulting in the evaluation of 31 patients (32 shoulders). The surgical indications encompassed cuff tear arthropathy (CTA) in 20 shoulders, omarthrosis (OA) in 7, post-traumatic deformity (PTD) in 3, rheumatoid arthritis (RA) in 2, osteochondrodysplasia (OCD) in 1, and psoriatic arthritis (PA) in 1. Among the patient cohort, there were 20 females and 11 males, with a mean age of 67.2 years (± 8.8 years, ranging from 42 to 82) and a mean BMI 29.1 (± 5.5, ranging from 17.7 to 45.8) at the time of surgery. All patients underwent implantation of a RTSA using SMR Reverse Shoulder System (Lima Ltd, San Daniele del Friuli, Italy).

4.3 Musculoskeletal Model and Kinematics

We utilized the musculoskeletal model of the human shoulder (Fig. 9) proposed by Seth et al., 2019 [39]. This model, implemented in the OpenSim software, consisting of 16 muscles (33 muscle segments) integrates a swift and precise skeletal representation of scapulothoracic kinematics, as introduced by Seth et al., 2016 [40].

Three muscles, namely the subscapularis, supraspinatus, and long head of the biceps brachii, were deemed inadequate for inclusion in the musculoskeletal model. In cuff tear arthropathy, a prevalent indication for RTSA, the subscapularis and supraspinatus muscles often face irreparable conditions [41]. Additionally, the long head of the biceps brachii is typically interrupted during surgery and subsequently reconstructed adjacent to the short head, diminishing its primary contributions to shoulder movement and stability [42].

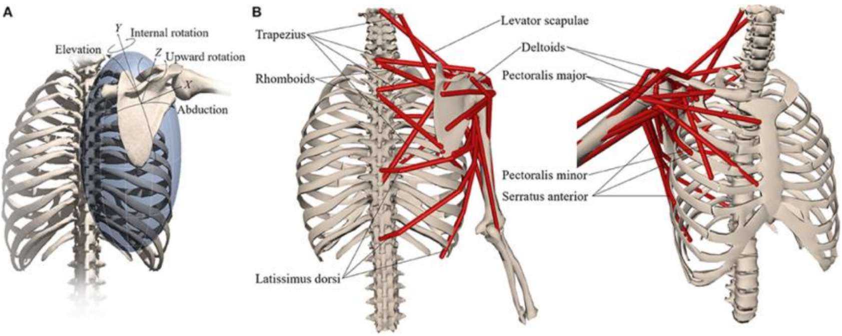

Fig. 9 Musculoskeletal model with (A) wrapping ellipsoid of thorax and scapula DOF and (B) selected muscles that control scapula [39].

The arm position in abduction and flexion was described by an elevation angle. Elevation angle is defined as an angle between the vertical and arm axis running through the COR of glenohumeral joint and the center of gravity of hand (Fig. 10). The motion in shrugging is described by vertical displacement of the COR of glenohumeral joint. The studied motions are described in Tab. 8.

Tab. 1 Description of studied motions, definition of coordinate frame is based on ISB recommendation for global coordinate system stated in Wu et al., 2005 [43].

Motion	**Description**	**Glenoid motion**
Abduction	Starting from neutral position, humerus abducted to 90° in the coronal plane; elbow fully extended	Rotation around x-axis
Flexion	Starting from neutral position, humerus abducted to 90° in the sagittal plane; elbow fully extended	Rotation around z-axis
Shrug	Starting from neutral position, shoulder raise; elbow fully extended	Translation in +y axis

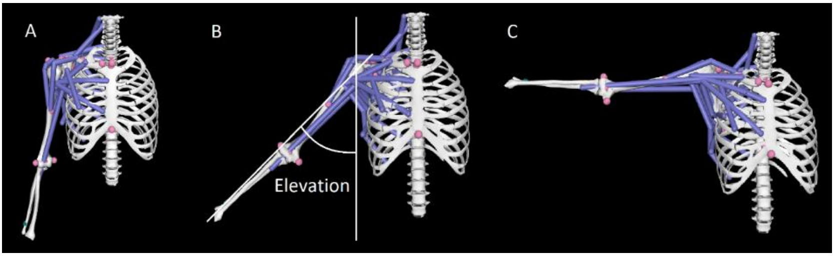

Fig. 10 Kinematics of abduction in OpenSim software in three positions: initial position (A), 45 degrees (B), and 90 degrees (C).

Local coordinate system of the humerus was used for evaluation of the changes in musculoskeletal geometry as shown in Fig. 11.

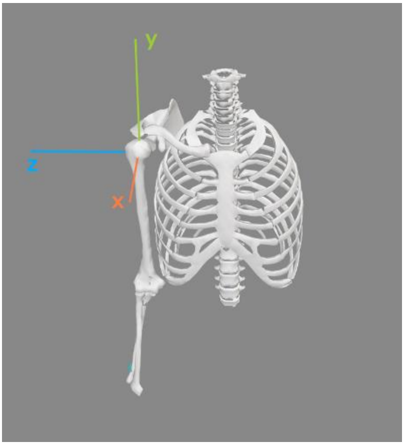

Fig. 11 The local coordinate system of humerus according to Wu et al., 2005 [43]. X-axis is in anterior-posterior meaning, y-axis is in superior-inferior meaning and z-axis in medialis-lateralis meaning.

4.4 Muscle Models

The principle of humerus prolongation is based on utilization of passive muscle response in order to improve RTSA stability. However, different biomechanical studies adopt diverse muscle models. To assess the impact of the muscle model on the predicted glenohumeral load, we employed various muscle models. Three Hill-type muscle models comprising three elements (Fig. 12) – Thelen, 2003 [44], McLean et al., 2003 [45], Geyer et al., 2003 [46] and one Hill-type muscle model comprising four elements – Haeufle et al., 2014 [47].

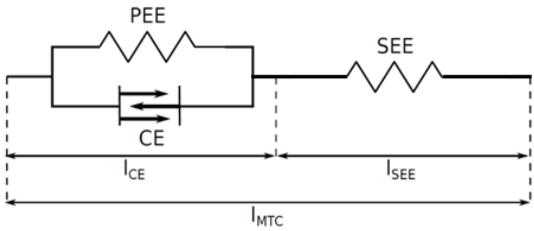

Fig. 12 The configuration of the three elements MTC

The kinematics of the movements were addressed by employing slow movements, allowing for a quasi-static analysis of slow motion. Consequently, parameters associated with contraction velocity could be disregarded.

All the muscle tendon complexes (MTC) consist of active (muscle) and passive (tendon) part. The active part includes contractile element (CE), responsible for active force production and parallel elastic element (PEE), aligned parallel to the CE and which simulates passive response of the muscle fibres. The passive part includes serial elastic element (SEE), positioned in series with the CE and simulating the elastic response of tendon. The pennation angle was applied to all muscle models by multiplying the resultant force by the cosine of the pennation angle.

Forces in the MTCs are F_{max}, maximum isometrical force (optimized parameter), F_{CE}, contractile element force (calculated), F_{SEE}, serial element force (calculated), F_{PEE}, parallel element force (calculated), and F_M, total muscle force (calculated). Together, these elements uphold force equilibrium as shown in equation (2).

$$F_M = F_{CE} + F_{PEE} = F_{SEE} \tag{2}$$

Lengths in the MTCs are l_{MTC}, total muscle tendon complex length (calculated), l_{CE}, contractile element length (calculated) initialized to l_{CE}^{opt}, optimal contractile element length (optimized parameter), l_{SEE}, serial element length (calculated), l_{PEE}, parallel element length (calculated), l_{CE}^{slack}, muscle slack length (optimized parameter), l_{SEE}^{slack}, tendon slack length (optimized parameter). The kinematic relations in MTC between the elements are shown in equations (3) and (4).

$$l_{PEE} = l_{CE} \tag{3}$$

$$l_{MTC} = l_{SEE} + l_{CE} \tag{4}$$

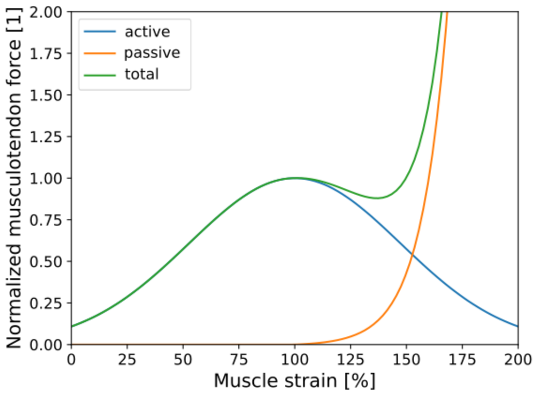

Fig. 13 Force-length relation of the contractile element (CE, blue line) and the parallel elastic element (PEE, orange line) in Thelen, 2003 [45] muscle model. Green line indicates total muscle force. Data is shown for middle deltoid with 100 % activation.

4.5 Estimation of Glenohumeral Load and Simulation of Humeral Lengthening

The estimation of glenohumeral load was conducted through a mathematical model that considers the equilibrium of forces and torques within the joint. Muscles were represented as active fibers running from proximal to distal attachment points. Muscle paths, including wrapping points, were aligned with moment arms estimated from cadaver experiments (Ackland et al., 2008 [48]). Effective moment arms and muscle vectors were derived from OpenSim (version 4.1) using the MuscleForceDirection plugin, while the musculotendon length was obtained using MuscleAnalysis tool. Segment masses were extracted from an arm reference model described by Wu et al., 2016 [49] and center of gravity positions were sourced from a model by Seth et al., 2019 [39].

During motion, gravitational torques on individual body segments were balanced by muscle actions.

A static biomechanical analysis was employed, deemed acceptable for slow motions where the velocity of body parts could be neglected. This approach facilitated the comparison of individual trials at specific body positions. The glenohumeral joint was estimated using both passive and active approaches. In the former, muscle activation was set to zero, and muscle force was generated by nonlinear springs of parallel and serial elastic elements. In the latter, addressing the issue of muscle redundancy involved solving equilibrium torques in the shoulder joint. The model, with more active muscle forces than torque equilibrium equations, was statically indeterminate. Optimization, using the sum of squared muscle activation as the criterion [50], was employed, considering equilibrium torque equations and muscle force generation capacity as constraints. Muscle force generation was influenced by musculotendon length, with muscle fiber and tendon lengths calculated for each muscle based on force and deformation transmission in the hill model at a given level of activation. Consequently, glenohumeral force was derived from the force equilibrium of the upper extremity [IX].

The generic musculoskeletal model underwent modifications to account for changes in humeral geometry after RTSA [II]. The adjustments involved considering alterations in the rotation of the glenoidal joint, as well as changes in the position and length of the humerus. Rotational alteration was implemented by adjusting the position of the COR in the glenohumeral joint (Fig. 14). For humerus lengthening, adjustments were made to the muscle attachment points by introducing a vector representing humeral displacement to the original attachment points in the humerus coordinate system [43] (Fig. 15).

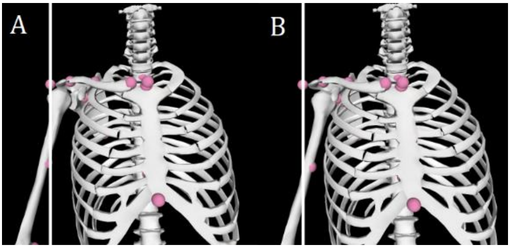

Fig. 14 Vizualization of medial shift of COR according to acromial marker. Shown in neutral position (A) and shifted medialy after RTSA (B).

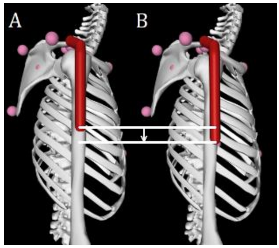

Fig. 15 Vizualization of humeral prolongation shown on middle deltoideus. Shown in neutral position (A) and prolonged after RTSA (B).

4.6 Statistical analyses

Data analysis was performed utilizing R (R Foundation for Statistical Computing, Vienna, Austria, version 4.1.2). To assess inter-observer variability, the intra-class correlation coefficient (ICC) was calculated using model 2.1 as described by Shrout and Fleiss [51]. The Shapiro-Wilk test was employed to assess the normal distribution of data. The analysis was conducted for the entire cohort as well as separately for male and female patients. The Welch Two Sample t-test and one way analysis of variance (ANOVA) followed by Tukey’s post hoc test for normally distributed data were used to evaluate the differences between cohorts. Multiple linear regression was employed to investigate whether patients' weight and height significantly predicted magnification [52]. The computation of 95% confidence intervals (CIs) and p-values was carried out using the Wald approximation. An alpha of 0.05 was applied for evaluating statistical significance. In the post-hoc power analysis, based on the sample size for the primary outcome, the power was determined to be 0.99 for a two-tailed comparison, with an effect size of 0.5 and an α error of 0.05.

A Pearson correlation coefficient was computed to assess the linear relationship between humeral prolongation and age, humeral prolongation and BMI, humeral prolongation and height, and humeral prolongation and weight. Correlations between patient characteristics and measured changes in musculoskeletal geometry were also evaluated using Pearson correlation coefficients.

5 Results

5.1 Radiographical Magnification in Shoulder Joint Region

There was an excellent agreement between the observers in evaluation the magnification of radiographs (inter-rater ICC = 0.997, 95% confidence interval 0.991-0.999). The average magnification factor was 11.91% (standard deviation 3.24%, range 5.74%–20.31%) [I, V]. The magnification factor was normally distributed (Shapiro-Wilk normality test p = 0.209) as shown in Fig. 16.

A slightly higher radiographic magnification was observed in male (mean 12.7%, standard deviation 3.5%) than in female patients (mean 11.4%, standard deviation 3.1%), the difference was not significant (Welch Two Sample t-test p=0.077). A linear model was fitted to predict radiographic magnification with patients' height and weight. The model's explanatory power is weak (R = 0.09) indicating large inter-individual variability among patients (Fig. 17). The effect of weight is statistically significant and positive (p = 0.017), while the effect of height is statistically non-significant (p = 0.648) [I, V].

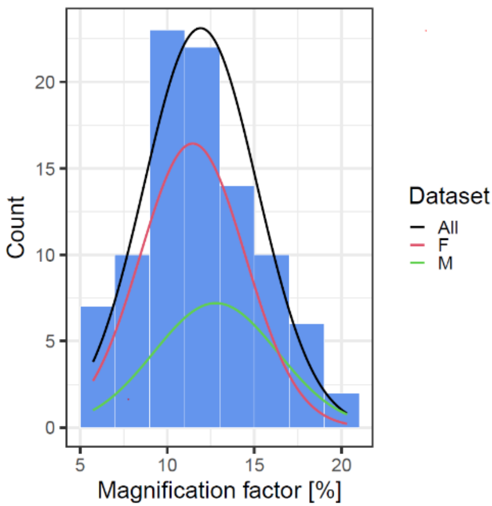

Fig. 16 Histogram of magnification factor for all patients and fitted Gaussian curves for all patients (All), female (F) and male (M) [I].

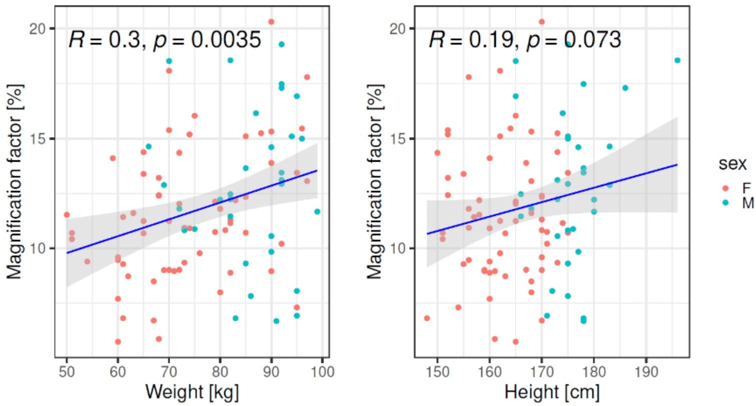

Fig. 17 Linear regression model (highlighted in blue) and a 95% confidence area (shaded area) illustrating the association between patients' weight (left) and height (right) with the magnification factor across all patients. In each plot, the Pearson correlation coefficient and corresponding p-value are provided to quantify the strength and significance of the observed relationships [I].

5.2 Changes in Musculoskeletal geometry after RTSA

Three changes of musculoskeletal geometry after RTSA were determined as shown in Fig. 49. The average shift of COR was 19.9 mm medially (standard deviation 7.9 mm, range 2.9–36.9 mm) and 6.2 mm inferiorly (standard deviation 7.4 mm, range -11.6–18.3 mm) [IV]. The medial and inferior shift of COR was normally distributed among patients (Shapiro-Wilk normality test W = 0.98139, p = 0.839 and W = 0.96839, p = 0.4562, respectively) as shown in Fig. 18.

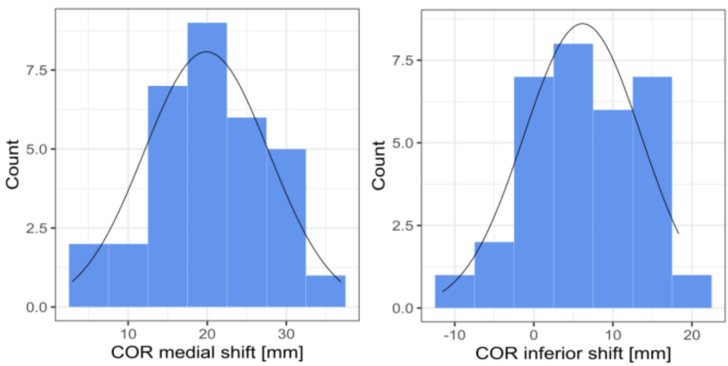

Fig. 18 Histogram of COR shift for all patients and fitted Gaussian curve.

The average prolonging of humerus in the direction of longitudinal axis of the humerus was 15.2 mm (standard deviation 6.2 mm, range 1.8–30.6 mm) and in lateral meaning (perpendicularly to the longitudinal axis of humerus) 11.8 mm (standard deviation 4.5 mm, range 1.3–17.9 mm), which resulted in average total prolonging of 19.7 mm (standard deviation 6.4 mm, range 2.2–35.2 mm) [III]. The inferior, lateral, and total prolonging of humerus was normally distributed among patients (Shapiro-Wilk normality test $W = 0.98857$, $p = 0.9774$; $W = 0.92197$, $p = 0.02352$; and $W = 0.97215$, $p = 0.5606$, respectively) as shown in Fig. 19. The distribution of data in humerus lateral shift might be influenced by the geometry of the replacement [VII].

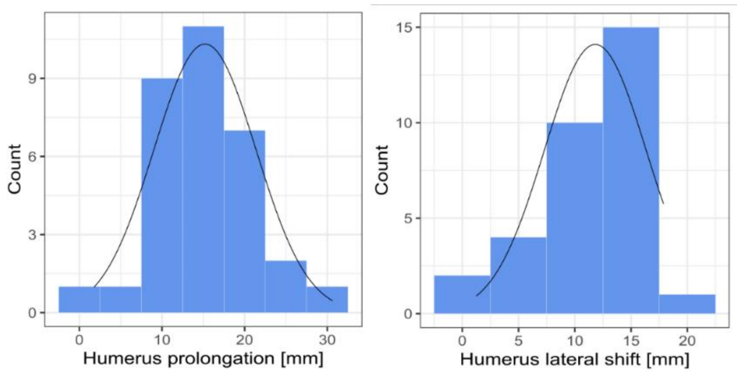

Fig. 19 Histogram of humerus prolongation and lateral shift for all patients and fitted Gaussian curves.

5.3 Influence of Muscle Model on Glenohumeral Joint Load

To assess the impact of muscle models on glenohumeral joint load, four different muscle models were employed in three distinct motions. Both passive and active motions were used to evaluate reaction forces, with passive motion representing no muscle activity and no gravitational influence, assessing passive forces alone. Active motion reflected real motion with the weights of body segments and active muscle engagement. The influence of the muscle model was evaluated with the glenohumeral joint in its anatomical position for comparability with existing literature. As depicted in Fig. 20 for abduction, the choice of muscle model significantly impacted glenohumeral joint load. The highest load in all movements occurred when employing the Haeufle et al., 2014 [47] muscle model, while the lowest forces were observed with the

Thelen, 2003 [44] muscle model. Although the muscle models showed the same qualitative trend, they varied quantitatively [XI].

Based on these results, the Thelen, 2003 [44] muscle model was chosen as a reference for all subsequent evaluations due to its widespread citation and close resemblance to in vivo measurements by Bergmann et al., 2007 [37] and Bergmann et al., 2011 [38].

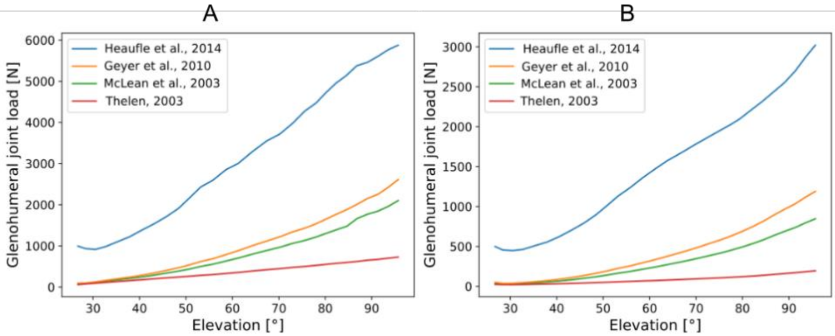

Fig. 20 The effect of formulation of Hill-type muscle model on glenohumeral joint load during active abduction (A) and passive abduction (B) [XI].

5.4 Influence of RTSA on Glenohumeral Joint Load

We assessed the influence of the actual surgery on glenohumeral joint load. To evaluate post-surgery data, a virtual surgery was performed using the average outcomes of a clinical study we conducted. This involved a medial shift of the COR by 19.9 mm and an inferior shift by 6.2 mm, along with humeral prolongation by 15.2 mm in the longitudinal axis direction and lateral shift by 11.8 mm perpendicular to the longitudinal axis [III]. Additionally, subscapularis, supraspinatus, and the long head of the biceps brachii were excluded. The data before surgery corresponds to the anatomical position of the glenohumeral joint with all muscles engaged.

The impact of RTSA on muscle force in each muscle during active abduction, considered as a reference motion according to literature, was also assessed (Fig. 21). The most substantial impact of RTSA on muscle forces was observed in the middle deltoid, where the force was approximately halved compared to the anatomical shoulder. Conversely, the surgery had the opposite effect on the coracobrachialis, showing increased muscle force after RTSA, but the absolute difference was significantly lower than the decrease in muscle force observed in the middle deltoid. In the long head of the triceps brachii, it could be observed that RTSA initially prolonged the muscle at the beginning of abduction, but at 90 degrees of abduction, the muscle force mirrored that of the anatomical shoulder. The effect of RTSA on the other muscles was not significant [IX].

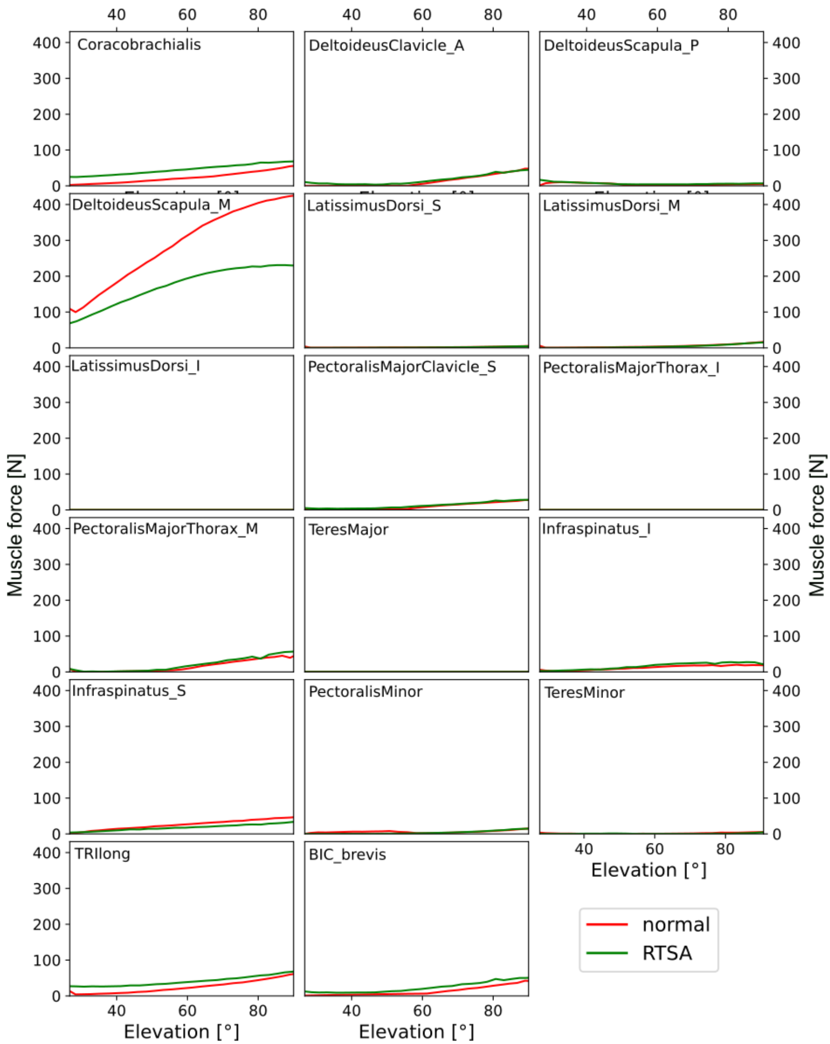

Fig. 21 Effect of RTSA on muscle force in each muscle during active abduction [IX].

5.5 Influence of RTSA Humerus Prolongation on Glenohumeral Joint Load

The effect of change of position of humerus after RTSA was assessed according to its prolongation and lateralization on glenohumeral joint load. The results were calculated with COR of glenohumeral joint in shifted position as was evaluated from our clinical study of RTSA patients, indicating a medial shift of 19.9 mm and an inferior shift of 6.2 mm [I, V]. Both active and passive motions were assessed at 30°, 60°, and 90° for abduction and forward flexion. A safe zone for humerus prolongation during RTSA was determined to prevent overloading the glenohumeral joint during these motions. The negative value in the meaning of x-axis stands for medialization and positive for lateralization in Figs 22–24. In the meaning in y-axis, the negative values mean shortening of humerus and positive stand for prolongation.

In 30 degrees of abduction (Fig. 22) the highest glenohumeral joint loads could be observed compared to 60 and 90 degrees of abduction. Based on the glenohumeral joint load in anatomical shoulder during abduction (around 800 N), counting this value as a margin of safe zone, a prolongation of around 25 mm with lateral or medial shift around 20 mm is possible. Lateralization was observed as more favourable than medialisation [III].

In 60 degrees of abduction (Fig. 23), the estimated safe zone was nearly 35 mm for humerus prolongation, with minimal impact from lateralization or medialization within the evaluated range of -20–20 mm [III].

In 90 degrees of abduction (Fig. 24) the observed safe zone for humerus prolongation was similar to that at 30 degrees (around 25 mm). In the sagittal plane, the shift showed opposite behaviour compared to 30 degrees, with medialization being slightly more favourable than lateralization [III].

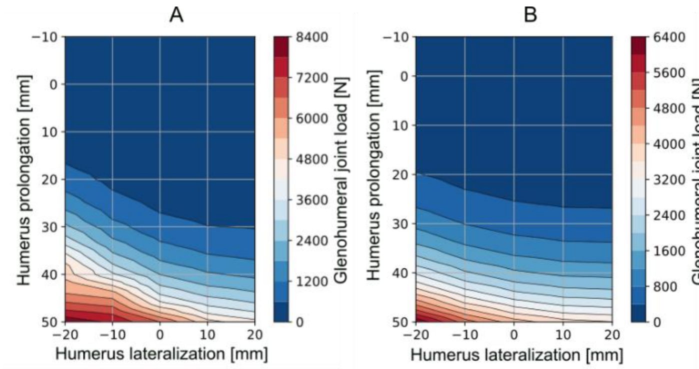

Fig. 22 Determination of the safe zone based on humerus prolongation and lateralization in RTSA. Shown in 30 degrees of active abduction (A) and passive abduction (B) [III].

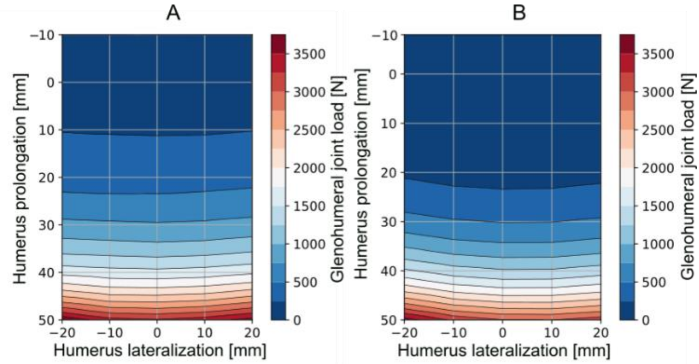

Fig. 23 Determination of the safe zone based on humerus prolongation and lateralization in RTSA. Shown in 60 degrees of active abduction (A) and passive abduction (B) [III].

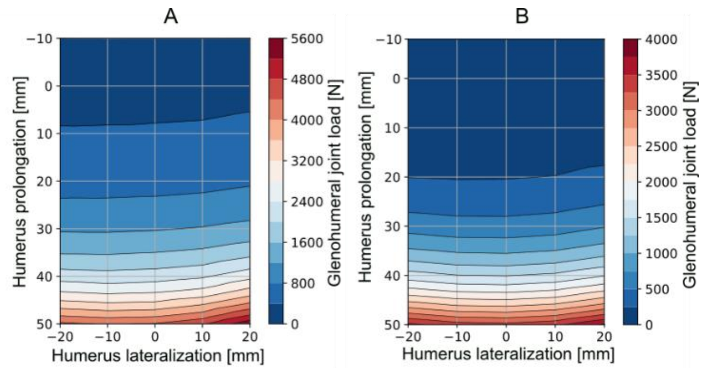

Fig. 24 Determination of the safe zone based on humerus prolongation and lateralization in RTSA. Shown in 90 degrees of active abduction (A) and passive abduction (B) [III].

The impact of humerus prolongation on each muscle force is illustrated in Fig. 25. Humerus prolongation resulted in the pre-stressing of shoulder muscles, generating a load that participates on stabilizing the joint. The muscles most affected include the deltoid, particularly its middle part, coracobrachialis, pectoralis major, long head of triceps brachii, and short head of biceps brachii.

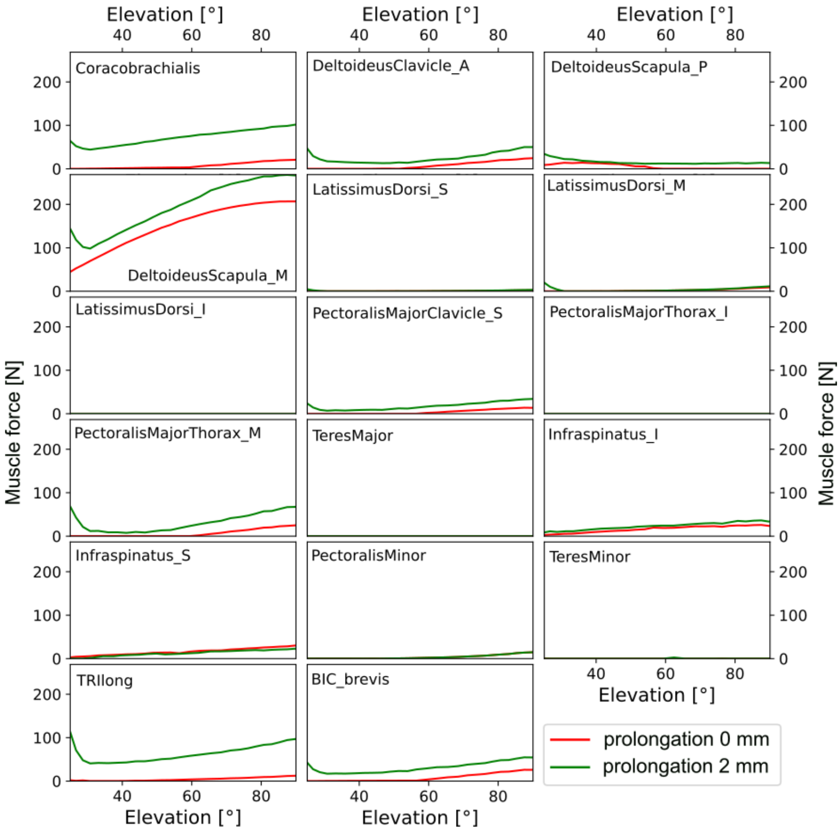

Fig. 25 Muscle forces in each muscle during active abduction, with 0 and 2 mm of humerus prolongation [III].

6 Conclusions

The shoulder joint, responsible for numerous activities in daily living, stands out as the most mobile joint within the human body. Utilizing a biomechanical approach can provide insights into the roles of individual anatomical structures in a healthy shoulder and offer suitable treatment options for pathological conditions. In this thesis, our focus lies on the clinical analysis of reverse total shoulder arthroplasty.

The accuracy of biomechanical model depends on the accuracy of the input data [II]. As most of the data is obtained from plain radiographs, we have studied the range of radiographic magnification and its variability among patients. In a clinical study of 94 patients, the real magnification measured from plain radiographs taking joint replacement as a marker, was approximately 12% (ranging from 5% to 20%) [I, V]. This value considerably differs from value of 5% proposed by replacement producer and implemented in the surgery planning software [I, V].

The knowledge of actual magnification played a crucial role in a subsequent study of humerus prolongation, employing a novel algorithm that integrates data from plain radiographs and CT scans. [VI, VIII]. This approach not only reduced radiological exposure of a patient in a prospective study but also enabled the utilization of archived data in a retrospective study involving 32 shoulders. Our findings revealed an average humerus prolongation of 15.2 mm (ranging from 1.8 mm to 30.6 mm), a dimension not previously reported [III].

The effect of humerus prolongation was studied in a comprehensive shoulder model [X, XI]. Exploring the impact of humerus prolongation, we employed a comprehensive shoulder model. Our research demonstrated that RTSA contributes to lower muscle force in the middle deltoid, a primary abductor, and glenohumeral joint load. [IV, VII]. However, extensive humerus prolongation (greater than 3 cm) could increase glenohumeral joint load more than three times [III, IX]. Consequently, we defined a safe zone for humerus prolongation in RTSA that should be considered during surgical procedures. [III].

7 References

[1] BRUIJN, S. M.; MEIJER, O. G.; BEEK, P. J. and VAN DIEËN, J. H. The effects of arm swing on human gait stability. online. *Journal of Experimental Biology*. 2010, ed. 213, iss. 23, p. 3945-3952. ISSN 1477-9145.

[2] EATHER, N.; WADE, L.; PANKOWIAK, A. and EIME, R. The impact of sports participation on mental health and social outcomes in adults: a systematic review and the 'Mental Health through Sport' conceptual model. online. *Systematic Reviews*. 2023, ed. 12, iss. 1. ISSN 2046-4053.

[3] SHEEAN, A. J; DE BEER, J. F; DI GIACOMO, G.; ITOI, E. and BURKHART, S. S. Shoulder instability: State of the Art. online. *Journal of ISAKOS*. 2016, ed. 1, iss. 6, p. 347-357. ISSN 20597754.

[4] BURNER, T.; ABBOTT, D.; HUBER, K.; STOUT, M.; FLEMING, R. et al. Shoulder Symptoms and Function in Geriatric Patients. online. *Journal of Geriatric Physical Therapy*. 2014, ed. 37, iss. 4, p. 154-158. ISSN 1539-8412.

[5] CRIMMINS, E. M. Lifespan and Healthspan: Past, Present, and Promise. online. *The Gerontologist*. 2015, ed. 55, iss. 6, p. 901-911. ISSN 0016-9013.

[6] SAMOUEI, R. and KEYVANARA, M. Identifying strategies for dealing with the aging population from the perspective of health system experts: A qualitative study. online. *Journal of Education and Health Promotion*. 2022, ed. 11, iss. 1. ISSN 2277-9531.

[7] GARVING, Ch.; JAKOB, S.; BAUER, I.; NADJAR, R. and BRUNNER, U. H. Impingement Syndrome of the Shoulder. online. *Deutsches Ärzteblatt international*. 2017. ISSN 1866-0452.

[8] LIN, D. J.; WONG, T. T. and KAZAM, J. K. Shoulder Arthroplasty, from Indications to Complications: What the Radiologist Needs to Know. online. *RadioGraphics*. 2016, ed. 36, iss. 1, p. 192-208. ISSN 0271-5333.

[9] BEST, M. J.; AZIZ, K. T.; WILCKENS, J. H.; MCFARLAND, E. G. and SRIKUMARAN, U. Increasing incidence of primary reverse

and anatomic total shoulder arthroplasty in the United States. online. *Journal of Shoulder and Elbow Surgery*. 2021, ed. 30, iss. 5, p. 1159-1166. ISSN 10582746.

[10] DRAKE, G. N.; O'CONNOR, D. P. and EDWARDS, B. T. Indications for Reverse Total Shoulder Arthroplasty in Rotator Cuff Disease. online. *Clinical Orthopaedics & Related Research*. 2010, ed. 468, iss. 6, p. 1526-1533. ISSN 0009-921X.

[11] BOILEAU, P.; WATKINSON, D. J.; HATZIDAKIS, A. M. and BALG, F. Grammont reverse prosthesis: Design, rationale, and biomechanics. online. *Journal of Shoulder and Elbow Surgery*. 2005, ed. 14, iss. 1, p. 147-161. ISSN 10582746.

[12] GOMBERAWALLA, M. M. and SEKIYA, J. K. Rotator Cuff Tear and Glenohumeral Instability. online. *Clinical Orthopaedics & Related Research*. 2014, ed. 472, iss. 8, p. 2448-2456. ISSN 0009-921X.

[13] SCHAIRER, W. W.; NWACHUKWU, B. U.; LYMAN, S.; CRAIG, E. V. and GULOTTA, L. V. National utilization of reverse total shoulder arthroplasty in the United States. online. *Journal of Shoulder and Elbow Surgery*. 2015, ed. 24, iss. 1, p. 91-97. ISSN 10582746.

[14] KIM, J. Y.; RHEE, Y. G. and RHEE, S.-M. Clinical Outcomes after Reverse Total Shoulder Arthroplasty According to Primary Diagnosis. online. *Clinics in Orthopedic Surgery*. 2020, ed. 12, iss. 4. ISSN 2005-291X.

[15] HALL, S. J. *BASIC BIOMECHANICS*. SIXTH EDITION. McGraw-Hill, 2012. ISBN 978-0-07-337644-8.

[16] ČIHÁK, R. *Anatomie 1*. 2. pub. Praha: Grada Publishing, 2001. ISBN 80-7169-970-5.

[17] LEVANGIE, P. K. and NORKIN, C. C. *Joint Structure and Function: A Comprehensive Analysis*. Fourth Edition. F. A. Davis Company, 2005. ISBN 0–8036–1191–9.

[18] NEUMANN, D. A. *KINESIOLOGY OF THE MUSCULOSKELETAL SYSTEM: Foundations for Rehabilitation*. Second Edition. Mosby, Inc., 2010. ISBN 978-0-323-03989-5.

[19] DESHMUKH, A. V.; KORIS, M.; ZURAKOWSKI, D. and THORNHILL, T. S. Total shoulder arthroplasty: Long-term survivorship, functional outcome, and quality of life. online. *Journal of Shoulder and Elbow Surgery*. 2005, ed. 14, iss. 5, p. 471-479. ISSN 10582746.

[20] CUFF, D.; PUPELLO, D.; VIRANI, N.; LEVY, J. and FRANKLE, M. Reverse Shoulder Arthroplasty for the Treatment of Rotator Cuff Deficiency. online. *The Journal of Bone & Joint Surgery*. 2008, ed. 90, iss. 6, p. 1244-1251. ISSN 0021-9355.

[21] CHALMERS, P. N.; SLIKKER, W.; MALL, N. A.; GUPTA, A. K.; RAHMAN, Z. et al. Reverse total shoulder arthroplasty for acute proximal humeral fracture: comparison to open reduction–internal fixation and hemiarthroplasty. online. *Journal of Shoulder and Elbow Surgery*. 2014, ed. 23, iss. 2, p. 197-204. ISSN 10582746.

[22] MIZUNO, N.; DENARD, P. J; RAISS, P. and WALCH, G. Reverse Total Shoulder Arthroplasty for Primary Glenohumeral Osteoarthritis in Patients with a Biconcave Glenoid. online. *The Journal of Bone and Joint Surgery-American Volume*. 2013, ed. 95, iss. 14, p. 1297-1304. ISSN 0021-9355.

[23] KONTAXIS, A. and JOHNSON, G.R. The biomechanics of reverse anatomy shoulder replacement – A modelling study. online. *Clinical Biomechanics*. 2009, ed. 24, iss. 3, p. 254-260. ISSN 02680033.

[24] DE WILDE, L. F.; AUDENAERT, E. A. and BERGHS, B. M. Shoulder prostheses treating cuff tear arthropathy: A comparative biomechanical study. online. *Journal of Orthopaedic Research*. 2004, ed. 22, iss. 6, p. 1222-1230. ISSN 0736-0266.

[25] SIMOVITCH, R. W.; HELMY, N.; ZUMSTEIN, M. A. and GERBER, Ch. Impact of Fatty Infiltration of the Teres Minor Muscle on the Outcome of Reverse Total Shoulder Arthroplasty. online. *The Journal of Bone & Joint Surgery*. 2007, ed. 89, iss. 5, p. 934-939. ISSN 0021-9355.

[26] HERRMANN, S.; KÖNIG, Ch.; HELLER, M.; PERKA, C. and GREINER, S. Reverse shoulder arthroplasty leads to significant biomechanical changes in the remaining rotator cuff. online. *Journal of Orthopaedic Surgery and Research*. 2011, ed. 6, iss. 1. ISSN 1749-799X.

[27] GREINER, S.; SCHMIDT, Ch.; KÖNIG, Ch.; PERKA, C. and HERRMANN, S. Lateralized Reverse Shoulder Arthroplasty Maintains Rotational Function of the Remaining Rotator Cuff. online. *Clinical Orthopaedics & Related Research*. 2013, ed. 471, iss. 3, p. 940-946. ISSN 0009-921X.

[28] GERBER, C.; PENNINGTON, S. D. and NYFFELER, R. W. Reverse Total Shoulder Arthroplasty. online. *Journal of the American Academy of Orthopaedic Surgeons*. 2009, ed. 17, iss. 5, p. 284-295. ISSN 1067-151X.

[29] GUTIÉRREZ, S.; LUO, Z.-P.; LEVY, J. and FRANKLE, M. A. Arc of motion and socket depth in reverse shoulder implants. online. *Clinical Biomechanics*. 2009, ed. 24, iss. 6, p. 473-479. ISSN 02680033.

[30] LÄDERMANN, A.; WALCH, G.; LUBBEKE, A.; DRAKE, G. N.; MELIS, B. et al. Influence of arm lengthening in reverse shoulder arthroplasty. online. *Journal of Shoulder and Elbow Surgery*. 2012, ed. 21, iss. 3, p. 336-341. ISSN 10582746.

[31] INMAN, V. T.; SAUNDERS, J. B. dec M. and ABBOTT, L. C. Observations of the Function of the Shoulder Joint. online. *Clinical Orthopaedics and Related Research*. 1996, ed. 330, p. 3-12. ISSN 0009-921X.

[32] POPPEN, N. K. and WALKER, P. S. Forces at the glenohumeral joint in abduction. *Clinical Orthopaedics and Related Research*. 1978, ed. 1978, iss. 135, p. 165-170.

[33] VAN DER HELM, F. C. T. A finite element musculoskeletal model of the shoulder mechanism. online. *Journal of Biomechanics*. 1994, ed. 27, iss. 5, p. 551-569. ISSN 00219290.

[34] FAVRE, P.; SNEDEKER, J. G. and GERBER, Ch. Numerical modelling of the shoulder for clinical applications. online. *Philosophical Transactions of the Royal Society A: Mathematical, Physical and Engineering Sciences*. 2009, ed. 367, iss. 1895, p. 2095-2118. ISSN 1364-503X.

[35] TERRIER, A.; VOGEL, A.; CAPEZZALI, M. and FARRON, A. An algorithm to allow humerus translation in the indeterminate problem of shoulder abduction. online. *Medical Engineering & Physics*. 2008, ed. 30, iss. 6, p. 710-716. ISSN 13504533.

[36] SINS, L.; TÉTREAULT, P.; HAGEMEISTER, N. and NUñO, N. Adaptation of the AnyBody™ Musculoskeletal Shoulder Model to the Nonconforming Total Shoulder Arthroplasty Context. online. *Journal of Biomechanical Engineering*. 2015, ed. 137, iss. 10. ISSN 0148-0731.

[37] BERGMANN, G.; GRAICHEN, F.; BENDER, A.; KÄÄB, M.; ROHLMANN, A. et al. In vivo glenohumeral contact forces—Measurements in the first patient 7 months postoperatively. online. *Journal of Biomechanics*. 2007, ed. 40, iss. 10, p. 2139-2149. ISSN 00219290.

[38] BERGMANN, G.; GRAICHEN, F.; BENDER, A.; ROHLMANN, A.; HALDER, A. et al. In vivo gleno-humeral joint loads during forward flexion and abduction. online. *Journal of Biomechanics*. 2011, ed. 44, iss. 8, p. 1543-1552. ISSN 00219290.

[39] SETH, A.; DONG, M.; MATIAS, R. and DELP, S. L. Muscle Contributions to Upper-Extremity Movement and Work From a Musculoskeletal Model of the Human Shoulder. online. Frontiers in Neurorobotics. 2019, ed. 13. ISSN 1662-5218.

[40] SETH, A.; MATIAS, R.; VELOSO, A. P.; DELP, S. L. and REN, L. A Biomechanical Model of the Scapulothoracic Joint to Accurately Capture Scapular Kinematics during Shoulder Movements. online. *PLOS ONE*. 2016, ed. 11, iss. 1. ISSN 1932-6203.

[41] EDWARDS, T. B.; WILLIAMS, M. D.; LABRIOLA, J. E.; ELKOUSY, H. A.; GARTSMAN, G. M. et al. Subscapularis insufficiency and the risk of shoulder dislocation after reverse shoulder arthroplasty. online. *Journal of Shoulder and Elbow Surgery*. 2009, ed. 18, iss. 6, p. 892-896. ISSN 10582746.

[42] SELIM, N. M. and BADAWY, E. R. Consider Long Head of Biceps Tendon for Reconstruction of Massive, Irreparable Rotator Cuff Tear. Online. Arthroscopy Techniques. 2021, ed. 10, iss. 2, p. 457-467. ISSN 22126287.

[43] WU, G.; VAN DER HELM, F. C. T.; VEEGER, H. E. J.; MAKHSOUS, M.; VAN ROY, P. et al. ISB recommendation on definitions of joint coordinate systems of various joints for the reporting of human joint motion—Part II: shoulder, elbow, wrist and hand. online. *Journal of Biomechanics*. 2005, ed. 38, iss. 5, p. 981-992. ISSN 00219290.

[44] THELEN, D. G. Adjustment of Muscle Mechanics Model Parameters to Simulate Dynamic Contractions in Older Adults. online. *Journal of Biomechanical Engineering*. 2003, ed. 125, iss. 1, p. 70-77. ISSN 0148-0731.

[45] MCLEAN, S. G.; SU, A. and VAN DEN BOGERT, A. J. Development and Validation of a 3-D Model to Predict Knende Joint Loading During Dynamic Movement. online. *Journal of Biomechanical Engineering*. 2003, ed. 125, iss. 6, p. 864-874. ISSN 0148-0731.

[46] GEYER, H.; SEYFARTH, A. and BLICKHAN, R. Positive force feedback in bouncing gaits?. online. *Proceedings of the Royal Society of London. Series B: Biological Sciences*. 2003, ed. 270, iss. 1529, p. 2173-2183. ISSN 0962-8452.

[47] HAEUFLE, D. F. B.; GÜNTHER, M.; BAYER, A. and SCHMITT, S. Hill-type muscle model with serial damping and eccentric force–velocity relation. online. *Journal of Biomechanics*. 2014, ed. 47, iss. 6, p. 1531-1536. ISSN 00219290.

[48] ACKLAND, D. C.; PAK, P.; RICHARDSON, M. and PANDY, M. G. Moment arms of the muscles crossing the anatomical shoulder. online. *Journal of Anatomy*. 2008, ed. 213, iss. 4, p. 383-390. ISSN 0021-8782.

[49] WU, W.; LEE, P. V. S.; BRYANT, A. L.; GALEA, M. and ACKLAND, D. C. Subject-specific musculoskeletal modeling in the evaluation of shoulder muscle and joint function. online. *Journal of Biomechanics*. 2016, ed. 49, iss. 15, p. 3626-3634. ISSN 00219290.

[50] VAN VEEN, B.; MONTEFIORI, E.; MODENESE, L.; MAZZà, C. and VICECONTI, M. Muscle recruitment strategies can reduce joint loading during level walking. online. *Journal of Biomechanics*. 2019, ed. 97. ISSN 00219290.

[51] SHROUT, P. E. and FLEISS, J. L. Intraclass correlations: Uses in assessing rater reliability. online. *Psychological Bulletin*. 1979, ed. 86, iss. 2, p. 420-428. ISSN 0033-2909.

[52] FOX, J. *Applied Regression Analysis and Generalized Linear Models*. Third Edition. SAGE Publications, Inc, 2015. ISBN 9781452205663.

8 List of publications related to the dissertation

Articles

[I] **Kratochvíl, A.**; Daniel, M.; Fulín, P., Pokorný D. Radiographical magnification of the shoulder region. Online. *Obere Extremität*. 2024. doi: 10.1007/s11678-024-00802-x (IF 0.4)

[II] Votava J., **Kratochvíl A.**, Daniel M. Intra and inter-rater variability in the construction of patient-specific musculoskeletal model. Online. *Gait & Posture*. 2023. doi: 10.1016/j.gaitpost.2023.12.001. (IF 2.4)

[III] **Kratochvíl, A.**; Daniel, M.; Fulín, P., Walder J. The influence of humeral lengthening in reverse total shoulder arthroplasty on glenohumeral biomechanics. 2024. Submitted to The Journal of Bone and Joint Surgery.

Conference proceedings

[IV] **Kratochvíl, A.**; Daniel, M.; Fulín, P. ANALYSIS OF DISPLACEMENT OF CENTER OF ROTATION DURING REVERSE SHOULDER ARTHROPLASTY. In: 28th WORKSHOP OF APPLIED MECHANICS BOOK OF PAPERS. Praha: Czech Technical University in Prague, 2020. p. 42-44. ISBN 978-80-01-06791-8.

[V] **Kratochvíl, A.**; Daniel, M.; Fulín, P.; Pokorný, D. X-RAY MAGNIFICATION OF THE SHOULDER JOINT. In: 29th WORKSHOP OF APPLIED MECHANICS BOOK OF PAPERS. Praha: CTU FME. Department of Mechanics, Biomechanics and Mechatronics, 2021. p. 30-33. ISBN 978-80-01-06909-7.

[VI] **Kratochvíl, A.**; Daniel, M. Fitting postoperative 2D X-ray to preoperative 3D CT scan in patients with total shoulder arthroplasty. [Invited unpublished scientific lecture] 2022-11-11.

[VII] **Kratochvíl, A.**; Daniel, M.; Votava, J.; Pokorný, D.; Fulín, P. MECHANICS OF STABILIZATION IN REVERSE SHOULDER ARTHROPLASTY. In: 24th International Scientific Conference APPLIED MECHANICS 2023 BOOK OF ABSTRACTS. Bratislava: Strojnícka fakulta STU v Bratislave, 2023. ISBN 978-80-227-5294-7.

[VIII] **Kratochvíl, A.**; Daniel, M.; Fulín, P.; Walder, J. Metoda stanovení změn ve svalově-kosterní geometrii u pacientů s reverzní náhradou ramenního kloubu. In: XIV. mezinárodní konference BIOIMPLANTOLOGIE. Praha: Národní knihovna ČR, 2023. ISBN 978-80-11-03134-3.

[IX] **Kratochvíl, A.**; Daniel, M. Biomechanika reverzní náhrady ramenního kloubu. In: Human Biomechanics 2023 – Sborník. Praha: České vysoké učení technické v Praze, Fakulta strojní, 2023. ISBN 978-80-01-07179-3.

[X] **Kratochvíl, A.**; Daniel, M.; Fulín, P.; Walder, J. Pasivní odezva svalové tkáně u pacientů s reverzní náhradou glenohumerálního kloubu. In: Biomateriály a jejich povrchy XVI.. Praha: České vysoké učení technické v Praze, Fakulta strojní, 2023. 1.. ISBN 978-80-01-07212-7.

[XI] **Kratochvíl, A.**; Daniel, M. The Impact Of Varied Hill-Type Muscle Model Formulations On Glenohumeral Joint Loading. In: 25th International Scientific Conference APPLIED MECHANICS 2024 BOOK OF ARTICLES. Žilina: Faculty of Mechanical Engineering University of Žilina, 2024.